Journal of Alloys and Compounds 509 (2011) 9753–9757

Contents lists available at ScienceDirect

Journal of Alloys and Compounds

journal homepage: www.elsevier.com/locate/jallcom

Spectroscopic analysis of Nd^{3+}:$Ca_3Gd_2(BO_3)_4$ crystal and laser operating at 1.06 μm

Yuexia Ji[b], Yan Wang[a], Jiafeng Cao[b], Zhenyu You[a], Yeqing Wang[b], Chaoyang Tu[a,*]

[a] Key Laboratory of Photoelectric Materials Chemistry and Physics of CAS, Fujian Institute of Research on the Structure of Matter, Chinese Academy of Sciences, Fuzhou, Fujian 350002,China
[b] Graduate School of Chinese Academy of Sciences, Beijing City, 100039, China

ARTICLE INFO

Article history:
Received 9 March 2011
Received in revised form 25 July 2011
Accepted 4 August 2011
Available online 11 August 2011

PACS:
42.70.Hj
78.20.−e

Keywords:
Judd–Ofelt analysis
Optical properties
Laser operation

ABSTRACT

Laser crystal $Ca_3Gd_2(BO_3)_4$ of high quality activated with Nd^{3+} has been grown successfully by Czochralski technique. The product was characterized by means of X-ray diffraction (XRD) powder investigation. The absorption spectra along *a*-, *b*- and *c*-axes were measured and investigated according to the Judd–Ofelt theory. The fluorescence properties were pursued and the factors influencing the fluorescence quantum efficiency were indicated. Xe lamp-pumped pulsed laser results were also obtained and the highest output power was up to 62 mJ.

1. Introduction

Crystal hosts doped with Nd^{3+} ions have aroused researcher's interest in resent years due to the features surrounding 1.06 μm in the near IR wavelength. This wavelength, corresponding to the $^4F_{3/2} \rightarrow {}^4I_{11/2}$ transition, has been applied in practice, for example, as a visible wavelength from second harmonic generation [1]. Besides, Nd^{3+} is easily pumped to achieve the laser output, for the absorption band around 805 nm is well fitted to the emission of AlGaAs pump diodes.

$Ca_3Gd_2(BO_3)_4$ crystal belongs to orthorhombic system, in the space group of *Pnma* [2]. It melts congruently, so can be easily grown by the Czochralski method [3]. The good chemical, physics and optical properties make it an attractive crystal host in laser material research.

As we know, the optical properties along *a*-, *b*- and *c*-axes of the crystal and the laser operation have not been reported in recent years. In this research, we reported the growth progress and the optical properties of Nd^{3+}-doped $Ca_3Gd_2(BO_3)_4$ single crystal along the crystallographic axes which correspond to the refractive index axes in orthorhombic crystals (*a* is *x*-axis, *b* is *y*-axis and *c* is *z*-axis). An infrared laser output at 1.06 μm with Nd^{3+}:$Ca_3Gd_2(BO_3)_4$ crystal pumped by Xe lamp was also presented in this work.

2. Experimental procedures

Nd^{3+}:$Ca_3Gd_2(BO_3)_4$ single crystal of high quality (shown in Fig. 1) was obtained by Czochralski technique. The raw chemicals we used were $CaCO_3$ (analytical grade), H_3BO_3 (analytical grade), Gd_2O_3 (4 N purity) and Nd_2O_3 (4 N purity). The Nd^{3+}:$Ca_3Gd_2(BO_3)_4$ compound was synthesized by solid reaction, and Nd^{3+}:$Ca_3Gd_2(BO_3)_4$ single crystal (shown in Fig. 1) was grown along the *c*-axis in an iridium-crucible. The pulling and rotation rate were 1.0–1.5 mm/h and 13.0–20.0 rpm, respectively.

X-ray diffraction (XRD) investigation was used to demonstrate the crystal was $Ca_3Gd_2(BO_3)_4$. Fig. 2 shows the powder XRD pattern of Nd^{3+}:$Ca_3Gd_2(BO_3)_4$ recorded by Mini Flex II Desktop X-ray Diffractometer using Cu-K_α radiation (λ = 1.54059 Å). It is in agreement with the standard JCPDS card of $Ca_3Gd_2(BO_3)_4$ (JCPDS:48-0293), and a conclusion can be draw that the crystal we obtained was $Ca_3Gd_2(BO_3)_4$.

The samples used for the spectroscopic measurements were cut along *a*-, *b*- and *c*-axes of the crystal, then three pieces of samples were optically polished to flat and parallel faces with the thickness of 0.30 cm. The concentration of Nd^{3+} ions in the crystal was measured to be 0.99 wt% by the inductively coupled plasma-atomic emission spectrometry (ICP-AES) method and the corresponding Nd^{3+} concentration is 1.90912×10^{20} ions/cm^3. Room temperature absorption spectrum of each piece was recorded by Perkin-Elmer UV–vis–NIR spectrometer (Lambda-900). The room temperature fluorescence spectra and luminescent decay curve were also determined. The sample pumped by Xe lamp was cut and polished with a size up to diameter 4.0 × 55 mm^3. The output characteristics were determined in this research with Xe lamp-pumped pulsed laser.

* Corresponding author. Tel.: +86 591 8371 1368; fax: +86 591 8371 4946.
E-mail address: tcy@fjirsm.ac.cn (C. Tu).

0925-8388/$ – see front matter © 2011 Elsevier B.V. All rights reserved.
doi:10.1016/j.jallcom.2011.08.018

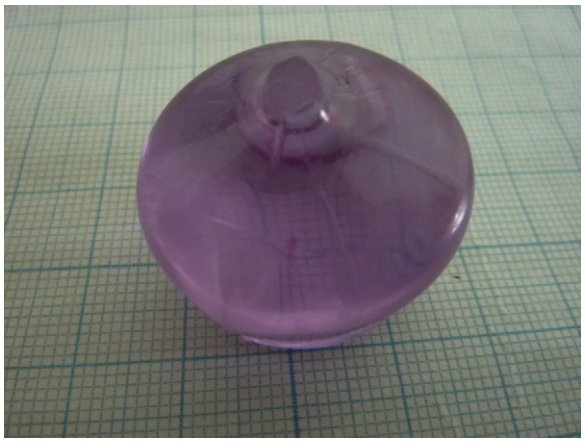

Fig. 1. Picture of the Nd^{3+}:$Ca_3Gd_2(BO_3)_4$ crystal.

3. Results and discussion

3.1. Absorption spectroscopy at room temperature

Room temperature absorption spectra along *a*-, *b*- and *c*-axes were shown in Fig. 3. About nine main absorption bands can be assigned in the range of 300–1000 nm corresponding to the transitions from ground $^4I_{9/2}$ level to $^4D_{1/2}+{}^4D_{3/2}+{}^4D_{5/2}$, $^2P_{1/2}$, $^2K_{13/2}+{}^2G_{11/2}$, $^4G_{7/2}+{}^4G_{9/2}+{}^2K_{13/2}$, $^4G_{5/2}+{}^2G_{7/2}$, $^4F_{9/2}$, $^4F_{7/2}+{}^4S_{3/2}$, $^4F_{5/2}+{}^2H_{9/2}$ and $^4F_{3/2}$ levels. The strong absorption bands at 805 nm are suitable for diode laser pumping. The mean value of the full width at half maximum (FWHM) at 805 nm is 14.26 nm, and the corresponding absorption cross-section were calculated to be 3.67×10^{-20} cm^2 according to the equation: $\sigma=\alpha/N_0$, where $\alpha=2.303A/L$ is the absorption coefficient, A is the absorbance, L is the thickness of the polished crystal, and N_0 is the concentration of Nd^{3+} in $Ca_3Gd_2(BO_3)_4$ crystal.

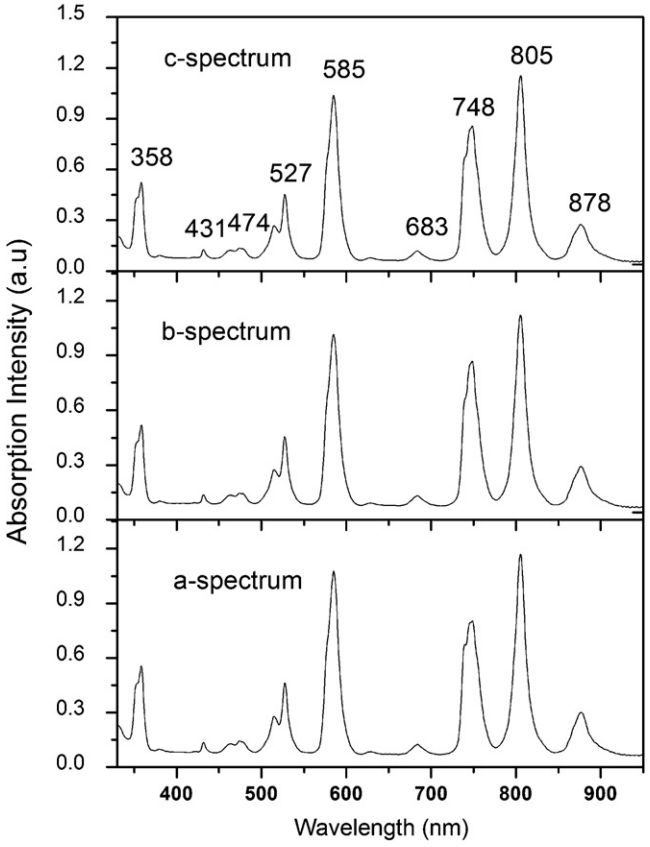

Fig. 3. Room temperature absorption spectra along *a*-, *b*- and *c*-axes of Nd^{3+}:$Ca_3Gd_2(BO_3)_4$.

3.2. The Judd–Ofelt analysis

The absorption spectra were used to calculate the optical parameters in the following research. The Judd–Ofelt (J–O) theory [4,5] was applied to analyze the spectroscopic properties

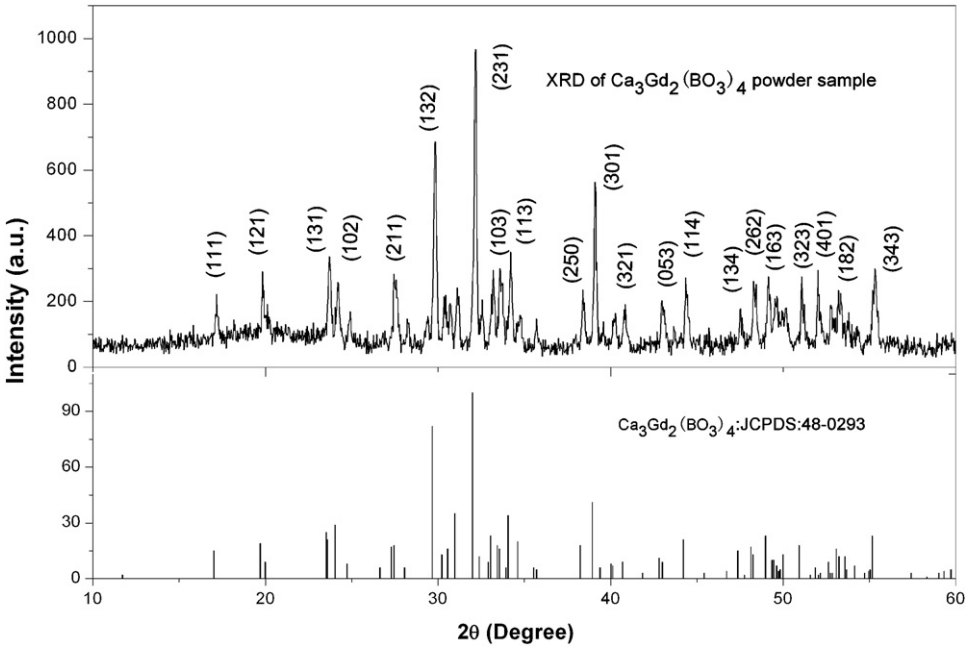

Fig. 2. X-ray diffraction pattern of $Ca_3Gd_2(BO_3)_4$ powder sample.

Table 1
The integrate absorbance, electrical dipole line strengths and the experimental oscillator strengths.

Excited states	$\bar{\lambda}$ (nm)	Γ (nm/cm) (average)	Line strength (10^{-20} cm^2)		Oscillator strength (10^{-6})	
			S_{exp}	S_{cal}	f_{exp}	f_{cal}
$^4D_{1/2}+{}^4D_{3/2}+{}^4D_{5/2}$	358	30.647	2.823	2.884	14.15	14.453
$^2P_{1/2}$	431	1.538	0.118	0.199	0.49	0.83
$^2K_{13/2}+{}^2G_{11/2}$	474	8.555	0.595	0.475	2.253	1.799
$^4G_{7/2}+{}^4G_{9/2}+{}^2K_{13/2}$	527	40.93	2.561	2.152	8.721	7.328
$^4G_{5/2}+{}^2G_{7/2}$	585	107.453	6.058	6.087	18.58	18.671
$^4F_{9/2}$	683	5.178	0.25	0.336	0.657	0.882
$^4F_{7/2}+{}^4S_{3/2}$	748	104.035	4.587	4.768	11.003	11.437
$^4F_{5/2}+{}^2H_{9/2}$	805	121.147	4.963	4.788	11.063	10.672
$^4F_{3/2}$	878	31.855	1.197	1.533	2.445	3.133

of Nd^{3+}:$Ca_3Gd_2(BO_3)_4$ single crystal, and the experimental line strength $S_{exp}(J-J')$ can be calculated by the following expression [6]:

$$S_{exp}(J-J') = \frac{3ch(2J+1)}{8\pi^3 N_0 \bar{\lambda} e^2} \frac{9n}{(n^2+2)^2} \Gamma(\bar{\lambda}) \quad (1)$$

where h is Planck's constant, J and J' are the total angular momentum of the ground state ($J=6$ in Nd^{3+}) and the angular momentum of the excited state, e is the value of the electronic charge, N_0 is the Nd^{3+} concentration in the crystal, c is the vacuum speed of light, $\bar{\lambda}$ is the mean wavelength of the absorption band, n is the mean value of refractive index of the $Ca_3Gd_2(BO_3)_4$ crystal, which is 1.77 according to Ref. [7]. The integrated absorbance $\Gamma(\bar{\lambda})$ for each absorption band can be obtained by:

$$\Gamma(\bar{\lambda}) = \frac{\int D(\lambda)d\lambda}{L \log e} = \frac{2.303 \int D(\lambda)d\lambda}{L}. \quad (2)$$

here $D(\lambda)$ is the measured optical density as a function of each wavelength and L is the sample thickness ($L=0.30$ cm).

According to the typical method of the Judd–Ofelt theory, the following equations were used to calculate line strengths for the $J \rightarrow J'$ line group:

$$S_{calc}(J \rightarrow J') = \Omega_2 U^{(2)}_{JJ'_n} + \Omega_4 U^{(4)}_{JJ'_n} + \Omega_6 U^{(6)}_{JJ'_n}, \quad (3)$$

$$U^{(t)}_{JJ'} = |\langle f^N \Psi J || U^{(t)} || f^N \Psi J' \rangle|^2, (t = 2, 4, 6). \quad (4)$$

where $U^{(t)}{}_{JJ'}$ ($t=2, 4, 6$) are the reduced matrix elements of tensor operators, given in Ref. [8]. When two absorption manifolds overlapped, the squared matrix element was taken to be the sum of the corresponding squared matrix elements. Three J–O intensity parameters Ω_t ($t=2, 4, 6$) were obtained by combining Eqs. (3) and (4), and the integrate absorbance and electrical dipole line strength were listed in Table 1.

The root mean square (rms) deviation between the experimental and calculated strengths was obtained by:

$$\mathrm{rms}\Delta S = \sqrt{\sum_{i=1}^{N} \frac{(S_{exp} - S_{calc})^2}{N-3}}. \quad (5)$$

here $N=9$ for Nd^{3+} is the number of absorption bands, and the root mean square (rms) deviation we pursued is 0.251×10^{-20} cm^2. The final experimental J–O parameters of Nd^{3+}:$Ca_3Gd_2(BO_3)_4$ we obtained were $\Omega_2 = 2.703 \times 10^{-20}$ cm^2, $\Omega_4 = 5.038 \times 10^{-20}$ cm^2 and $\Omega_6 = 6.881 \times 10^{-20}$ cm^2. Compared to 1.5% Nd^{3+}:YAG (2.71, 2.68 and 5.22×10^{-20} cm^2) [9], 1.5% Nd^{3+}:YAP (0.69, 3.69 and 4.56×10^{-20} cm^2) [10] and 3 at% Nd^{3+}:GAB (1.89, 4.41, 4.14×10^{-20} cm^2) [11], Nd^{3+}:$Ca_3Gd_2(BO_3)_4$ has higher values. Ω_2 is structure associated and sensitive with the asymmetry and covalence of the lanthanide sites. The high value of Ω_2 indicates there will be the low asymmetry and the strong covalence characteristics of Nd^{3+}:$Ca_3Gd_2(BO_3)_4$ crystal.

According to the theory, the experimental oscillator strength f_{exp} for a transition can be determined by using the following formula:

$$f_{exp} = \frac{mc^2 \Gamma}{\pi e^2 N_0 \bar{\lambda}^2}. \quad (6)$$

and the calculated oscillator strength f_{cal} can be obtained by:

$$f_{cal} = \frac{8\pi^4 mc}{3h(2J+1)\bar{\lambda}} \frac{(n^2+2)^2}{9n} \times \sum_{t=2,4,6} \Omega_t \langle 4f^N(\alpha', S', L')J' || U^t || 4f^N(\alpha, S, L)J \rangle^2 \quad (7)$$

The radiative decay rates $A(J \rightarrow J')$ is expressed below:

$$A(J \rightarrow J') = \frac{64\pi^4 e^2}{3h(2J+1)\overline{\lambda^3}} \frac{n(n^2+2)^2}{9} \times \sum_{t=2,4,6} \Omega_t |\langle (S, L)J || U^t || (S', L')J' \rangle|^2. \quad (8)$$

where U^t ($t=2, 4, 6$) are the reduced matrix elements of tensor operators, given in the Ref. [12]. The fluorescent branching ratio and the radiative lifetime are expressed by the following equations [13]:

$$\beta_{JJ'} = \frac{A(J \rightarrow J')}{\sum_{J'} A(J \rightarrow J')} \quad (9)$$

$$\tau_{rad} = \frac{1}{\sum_{J'} A(J \rightarrow J')} \quad (10)$$

According to our calculation, the values of $A_{JJ'}$, $\beta_{JJ'}$ and τ_{rad} were calculated, as shown in Table 2.

3.3. Fluorescence spectroscopy

The room temperature emission spectra of Nd^{3+}:$Ca_3Gd_2(BO_3)_4$ excited by 805 nm are shown in Fig. 4. About three bands can be observed from 800 nm to 1500 nm in the emission spectra corresponding to the $^4F_{3/2} \rightarrow {}^4I_{9/2}$, $^4I_{11/2}$, and $^4I_{13/2}$ transitions. A broad

Table 2
Calculated radiative transition rates, branching ratios radiative lifetimes and oscillator strength for different transition levels of Nd^{3+}:$Ca_3Gd_2(BO_3)_4$ crystal.

Transitions		$\bar{\lambda}$ (nm)	A (s^{-1})	β	τ (μs)
$^4F_{3/2}$	$^4I_{9/2}$	906	1931	0.373	193.04
	$^4I_{11/2}$	1062	2657	0.513	
	$^4I_{13/2}$	1337	562.6	0.109	
	$^4I_{15/2}$	1850	29.333	0.0057	

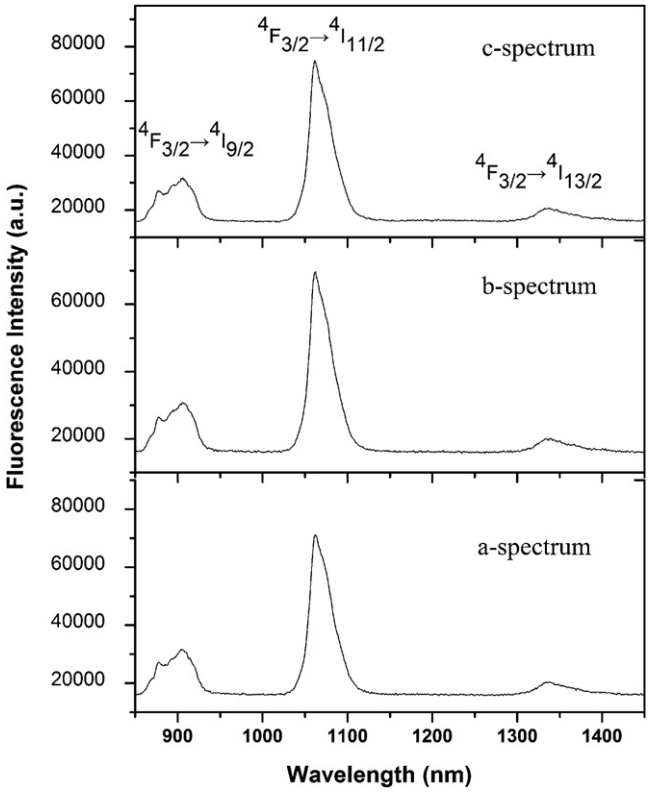

Fig. 4. Fluorescence spectra of Nd^{3+}:$Ca_3Gd_2(BO_3)_4$ crystal excited by 805 nm pumping.

band was observed from 1029 to 1125 nm, and it is possible to develop a tunable solid state laser in this wavelength region.

The Fuchtbauer–Ladengurg (F–L) formula [14] was used to calculate the emission cross-section, which was expressed by the following equation:

$$\sigma_{em}(\lambda) = \frac{\lambda^5 \beta}{8\pi c n^2 \tau_r} \frac{I(\lambda)}{\int [I(\lambda)]\lambda d\lambda}. \quad (11)$$

where λ is the vacuum wavelength of the emission peak and $I(\lambda)$ is the experimental emission intensity as a function of λ. The mean

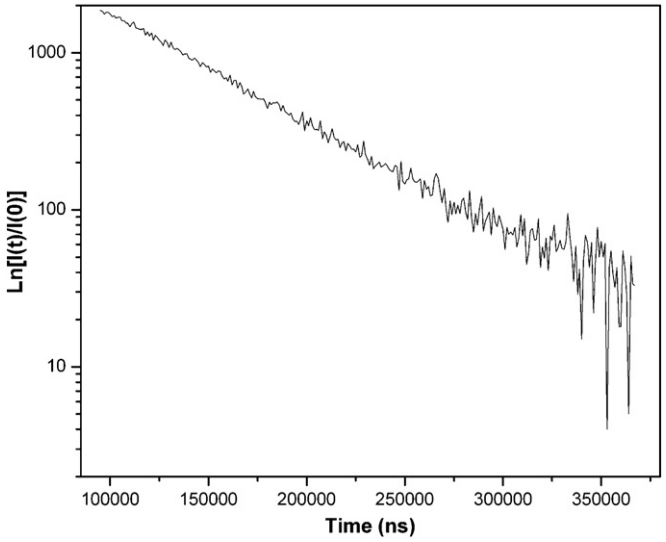

Fig. 5. Room temperature luminescence decay curve at 1062 nm excited by 805 nm pumping.

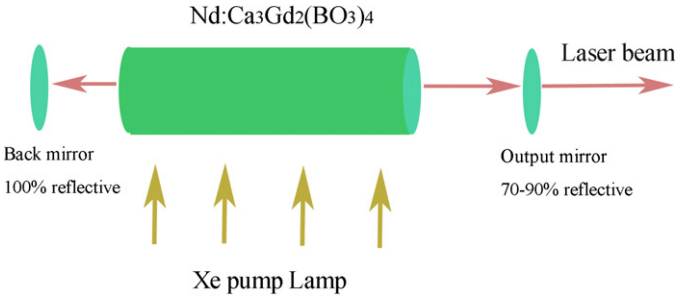

Fig. 6. Schematic of the experimental laser setup using Xe lamp as a pump source.

value of the emission cross-section at 1062 nm is 5.653×10^{-20} cm^2 according to our calculation.

The luminescent decay curve was recorded by FSP920 equipment with OPO laser pumping source. Fig. 5 shows the curve of the $^4F_{3/2} \rightarrow {}^4I_{11/2}$ transition excited by 805 nm at room temperature. The curve can be detected to be a single exponential behavior and the fluorescence lifetime can be understood by the curve: $I(t) = I(0)\exp(-At)$, where $I(t)$ and $I(0)$ are the fluorescence intensities corresponding to $t \neq 0$ and $t = 0$, A can be expressed by $A = 1/\tau$ and τ is the fluorescence lifetime. Thus the fluorescence lifetime of the $^4F_{3/2}$ manifold, $\tau = 1/A$, is estimated to be 62.4 μs. The quantum efficiency was calculated to be 32.3% according the equation $\eta = \tau_f/\tau_r$ for the $^4F_{3/2} \rightarrow {}^4I_{11/2}$ transition. The high phonon-energy laser host may be the main reason that prevents the quantum efficiency of the excited states of active ions, which will be discussed in the following sections.

3.4. Laser testing

Xe lamp was used as a pump source for the 1.06 μm laser performance study of Nd^{3+}:$Ca_3Gd_2(BO_3)_4$. The laser experiment was performed with a plano-plano cavity, as shown in Fig. 6.

The output power versus pumping power was shown in Fig. 7 with the laser test of Nd^{3+}:$Ca_3Gd_2(BO_3)_4$ rod corresponding to the transmissivity from 10% to 30%. The extremum of the output laser appeared when the pumping power is lager than 200 J, and a conclusion can be draw that the resonator with 20% output coupler transmissivity has the higher output (62 mJ) than the other at the pumping power at 230 J. The slop efficiency was up to 0.04% and the optical efficiency at 1062 nm was 0.034% with respect to

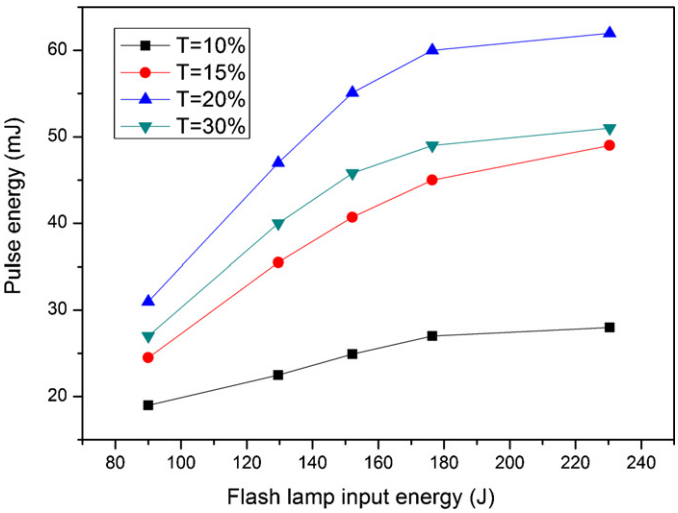

Fig. 7. Output power versus absorbed pump power of the Nd^{3+}:$Ca_3Gd_2(BO_3)_4$ laser pumped by Xe lamp.

the Xe lamp pump power. The possible corresponding reason for these low values was the existence of the high phonon energy in $Ca_3Gd_2(BO_3)_4$ crystal.

The effects of concentration quenching and multi-phonon relaxation are the main factors that reduce the rate of non-radiative transition in crystals. In Nd^{3+}-doped borates the fluorescence quenching is weak [15], and the rate of non-radiative transition in crystals is mainly caused by the effect of multi-phonon relaxation. The phonon energy of borate crystal is relatively higher compared to other crystals, and multi-phonon relaxation rate is relatively high. As a result, the fluorescence quantum efficiency of $^4F_{3/2}$ manifold in Nd^{3+}:$Ca_3Gd_2(BO_3)_4$ crystal is low, and the optical efficiency of 1.06 μm laser is lower than in other crystals hosts.

4. Conclusion

Nd^{3+}:$Ca_3Gd_2(BO_3)_4$ crystal with low defect has been grown by Czochralski technique in our lab. The spectroscopic study of Nd^{3+} ions in the $Ca_3Gd_2(BO_3)_4$ crystal has been displayed along three crystallographic physical-axes in this paper, and Judd–Ofelt theory was used in the absorption and fluorescence spectroscopy analysis. Xe lamp-pumping Nd^{3+}:$Ca_3Gd_2(BO_3)_4$ laser at 1062 nm was demonstrated, and the highest output power was up to 62 mJ. The low fluorescence quantum and the optical efficiency were mainly caused by the effect of the high value of phonon energy in $Ca_3Gd_2(BO_3)_4$ crystal.

Acknowledgements

This research was supported by National Nature Science Foundation of China (No. 50902129 and No. 61078076), Major Projects from FJIRSM (SZD08001-2 and SZD09001), Fund of Key Laboratory of Optoelectronic Materials Chemistry and Physics and Chinese Academy of Sciences (2008DP173016), Science and Technology Plan Major Project of Fujian Province of China (Grant No. 2010I0015) and Fund of Research Center of Laser Technology Integration and Application Engineering Technology of Haixi Industrial Technology Research Institute (2009H2009).

References

[1] A.A. Kaminskii, Laser Crystals, 2nd ed., Springer-Verlag, New York, 1990.
[2] C. Tu, Crystal growth, structure, optical spectra and laser properties of novel laser crystal, Doctor dissertation of Graduated School of Chinese Academy of Sciences, Fuzhou, 2004.
[3] B.V. Mill, A.M. Tkachuk, E.L. Belokoneva, Opt. Spectrosc. 84 (1998) 65.
[4] G.S. Ofelt, J. Chem. Phys. 37 (1962) 511.
[5] B.R. Judd, Phys. Rev. 127 (1963) 750.
[6] D. Jaque, O. Enguita, U. Caldino, M.O. Ramirez, J. Garcia Sole, J. Appl. Phys. 90 (2001) 561.
[7] P.H. Haumesser, R. Gaume, B. Viana, D. Vivien, J. Opt. Soc. Am. B 19 (2002) 2365.
[8] W.T. Carnall, P.R. Field, K. Rajnak, J. Chem. Phys. 49 (1968) 4424.
[9] W.F. Krupke, IEEE J. Quantum Electron. 7 (1971) 153.
[10] H. Zhang, Z.D. Luo, A. Zhang, J. Infrared Millimeter Waves 4 (1988) 297.
[11] G.F. Wang, J. Opt. Soc. Am. B 18 (2002) 173.
[12] P. Babu, C.K. Jayasankar, Physica B 301 (2001) 326.
[13] W.F. Krupke, IEEE J. Quantum Electron. 10 (1974) 450.
[14] B.M. Walsh, N.P. Barnes, B. Di Bartolo, J. Appl. Phys. 83 (1998) 2772.
[15] B.V. Mill, A.M. Tkachuk, E.L. Belokoneva, J. Alloys Compd. 277 (1998) 291.